COMFORT ASSESSMENT IN URBAN AIR MOBILITY VEHICLES

Aykut Tamer[†,*], Andrea Zanoni[‡], Pierangelo Masarati[‡]
[†]University of Bath, Department of Mechanical Engineering, BA2 7AY Bath - UK
[‡]Politecnico di Milano, Department of Aerospace Science and Technology, 20156 Milano - Italy
[*] at2849@bath.ac.uk

Abstract
Electric-powered flight is a promising solution to carbon emissions in aviation. Although still not feasible for mass transport, small-scale urban air mobility (UAM) vehicles already proved their feasibility for short-range missions. Their ancestor in terms of operational capabilities, the helicopter, is also known for high vibrational levels. While UAMs usually feature relatively small or slow rotors and/or propellers, meaning that dominant N_b/rev vibrations are expected to be of lower amplitude and higher frequency, they operate in conditions similar to those of helicopters. Besides, most UAMs are of unconventional architecture, which could lead to unanticipated vibrational issues. This work discusses how comfort assessment in UAMs may be approached by presenting a modular and versatile simulation environment.

Introduction

The aviation industry is pressed by an increasing demand for zero emissions. To answer it, substantial changes in the design of airframes, systems and propulsion must be developed and introduced in the market. One promising improvement is electric-powered flight, which has already proved its feasibility for short-range missions. Substantial increases in range require further advances in energy storage, but even with today's technology smart designs can provide new mobility models offering zero carbon emission. These missions are expected to be used in the transport of nine to fifty passengers in 60 min flights in the next decades [1]. Short-range requires vertical take-off and landing (VTOL) to avoid big airports in favour of dedicated terminals within cities, called *vertiports*.

Vibrations are an oscillatory response of the airframe to time-dependent loads. The predominant sources of vibration are the forces and moments originating from wings, rotors, engines, propellers, fuselage aerodynamics, engines and transmissions. The resulting time-dependent loads are transmitted to the fuselage, which excites the cockpit and the cabin. In helicopters, the current most popular VTOL-capable aircraft, vibrations are the main source of serious problems including reduced performance and increased maintenance costs [2, 3]. Severe vibratory levels can even cause structural failures and loss of control. Additionally, vibrations may also cause physiological and psychological reactions in the human body [4], which are felt by pilots, cabin crew, and passengers.

Although currently investigated UAM configurations typically lack a main rotor, and hence their vibratory loads are not expected to be as high as in helicopters, they will neither offer a ride experience as smooth as that of passenger jets since they will likely experience complex flight regimes analogous to those of helicopters, such as hover to forward-flight transition. Moreover, multiple powerplants will combine the effects of relatively low vibrational levels. Moreover, unconventional and diverse architectures of UAMs (Fig 1) are expected to introduce novel vibration-related problems. Therefore, UAMs are expected to face several vibration-related problems, mainly occupant comfort. To improve the understanding of the vibration exposure in UAM occupants, this work aims at building a numerical simulation framework that is capable to represent the complex physics of the problem while being flexible enough to support UAM design with a modular approach.

Figure 1: Urban air mobility concepts [5].

This work is organised as follows. The framework is described in the next chapter. Then, how to develop an example UAM model is explained, which includes an airframe, two wings carrying four engines and a human biodynamic model representing the pilot. Using the developed model, example analyses are conducted to demonstrate the usefulness of the method. The paper is completed with the conclusions and future work.

Method

The suggested method of efficient evaluation of comfort level in UAMs is composed of two steps. The first step is a modular simulation framework that allows versatility in generating overall vehicle models including the aircraft and human body. The second step is to post-process the results to include human perception of vibration.

High-Fidelity Modeling Environment

A multidisciplinary simulation environment favouring modularity is required to develop accurate and computationally efficient models of UAMs for moderate to high-frequency dynamic analysis. The model is thus obtained by assembling sub-components that represent the dynamics of different components: the sources of vibration, the path of transmission, the structural model of fuselage and cockpit, detailing the transmission of vibrations to occupants. Additionally, biomechanical models of the occupants are highly desirable to obtain a more realistic comfort level [6].

MASST (Modern Aeroservoelastic State Space Tools), a tool developed at Politecnico di Milano, was expressly designed for this purpose. It analyzes compact, yet complete modular models of linearized aeroservoelastic systems [7]. The subcomponents are collected from well-known, reliable and state-of-the-art sources (for example NASTRAN for airframe and CAMRAD for rotor). Then the individual models of the subcomponents are assembled using the Craig-Bampton Component Mode Synthesis (CMS) substructuring method [8], and cast in linear, time-invariant state-space form, defined by the quadruple $\mathbf{A}$, $\mathbf{B}$, $\mathbf{C}$, $\mathbf{D}$:

(1a) $$\dot{\mathbf{x}} = \mathbf{A}\mathbf{x} + \mathbf{B}\mathbf{f}$$

(1b) $$\mathbf{y} = \mathbf{C}\mathbf{x} + \mathbf{D}\mathbf{f}$$

where the vectors are defined as follows:

- $\mathbf{x}$ contains the states of the system, namely the degrees of freedom representing the system motion;
- $\mathbf{f}$ is the system input, namely the vibratory forces and moments applied by the vibration sources;
- $\mathbf{y}$ is the system output, namely the accelerations at selected locations.

Vibration Assessment:

The overall model evaluates acceleration at specified points. A generic acceleration can be expressed in the time domain (t) as:

(2) $$\mathbf{a}(t) = \begin{bmatrix} a_x(t) & a_y(t) & a_z(t) \end{bmatrix}^T$$

which refers to the acceleration of the human occupants. The acceleration can be measured at different points of the human body, which seems arbitrary. But ISO-2631 [9] suggests using the human contact point on the vibration surface. For typical aircraft use, this refers to human buttocks touching the seat cushion, which helps to relate the acceleration levels (measured or predicted) and comfort perception. For other applications, such as a recumbent person resting on a stretcher in a HEMS [10], other parts of the body can be used.

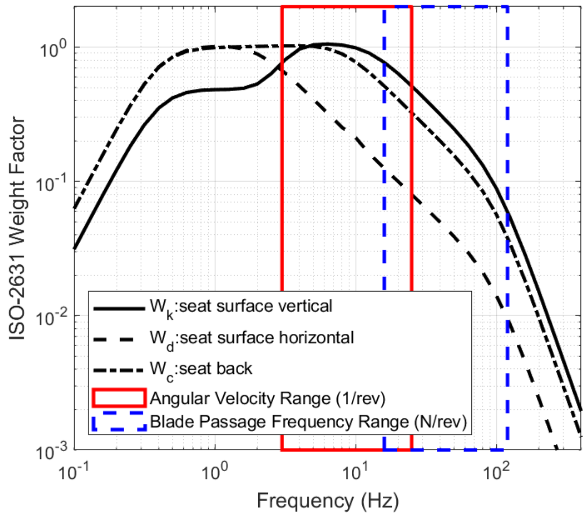

Figure 2: ISO comfort ratings [9] and typical angular speeds and blade passage frequencies of UAM propellers [11]. W_k: seat-surface vertical direction, W_d: seat-surface horizontal and lateral directions, W_c: seat-back.

ISO-2631 provides frequency weights to include the human perception of vibration, since human sensitivity changes with excitation frequency. For this purpose, frequency weights are suggested by standards such as ISO-2631. Fig. 2 presents the typical values of 1/rev and N_b/rev ranges over the human vibration sensitivity plots. The weight in this plot designates that the acceleration should be multiplied by that value to consider the human perception of vibration, so typically the values close to 1 mark the highest sensitivity. The figure shows that in different UAM vehicle concepts, the occupants can be exposed to accelerations at high sensitivity frequencies. To apply these weights, a discrete Fourier transform ($\mathfrak{F}$) is performed first:

(3) $$\mathfrak{F}(\mathbf{a}(t)) = \sum_{n=-\infty}^{\infty} \mathbf{A}(\omega_n) e^{j\omega_n t}$$

where $\mathbf{A}(\omega_n) = \{A_x(\omega_n); A_y(\omega_n); A_z(\omega_n)\}$ is the acceleration vector in the frequency domain. After applying the frequency ($W_d(\Omega_n)$, $W_k(\omega_n)$) and direction (k_x, k_y, k_z) weights dictated by ISO-2631, the frequency-weighted acceleration is formally given by

(4) $$\mathbf{a}_w = \sum_{n=-\infty}^{\infty} \begin{bmatrix} W_d(\omega_n)k_xA_x(\omega_n) \\ W_d(\omega_n)k_yA_y(\omega_n) \\ W_k(\omega_n)k_zA_z(\omega_n) \end{bmatrix} e^{j\omega_n t}$$

The ratings are given in terms of the root mean square (RMS) of the weighted acceleration magnitude over the exposure time T:

(5) $$a_{w,\text{RMS}} = \sqrt{\frac{1}{T}\int_0^T \mathbf{a}_w^T\mathbf{a}_w dt}$$

where for a sinusoidal acceleration at a single excitation frequency, the integral reduces to:

(6) $$a_{w,\text{RMS}} = \frac{1}{\sqrt(2)}|\mathbf{a}_w|$$

In case of multiple measurement points, the RMS magnitudes of the frequency-weighted accelerations at each location are collected in a vector:

(7) $$\mathbf{y} = [{}^ia_{w,1}\ {}^ia_{w,2}\ \ldots {}^ia_{w,j}\ \ldots\ {}^ia_{w,N}]^T$$

where ${}^ia_{w,j}$ is the frequency-weighted acceleration of the jth subject for $j = 1,..N$.

Given the averaged weighted magnitude of acceleration, ISO-2631 suggests a qualitative scale, as presented in Table 1. The effect of a vibration attenuation device can simply be evaluated by comparing the qualitative levels.

Table 1: Comfort rating after ISO-2631, converted to g at sea level.

Less than 0.03 g	not uncomfortable
0.03 g to 0.06 g	not comfortable
0.05 g to 0.10 g	a little uncomfortable
0.08 g to 0.16 g	fairly uncomfortable
0.13 g to 0.25 g	uncomfortable
Greater than 0.20 g	very uncomfortable

Analysis Model

A UAM model for comfort assessment requires a complete structural dynamics model of the aircraft. As this requires modelling the structure in detail that is usually confidential, there is no available aircraft data in the literature to demonstrate the comfort assessment of a UAM. For this purpose, the authors developed an aircraft model based on existing data obtained from different sources. An alternative would be to model a UAM structure from scratch but this would not make any difference for the scope of this work. Therefore, the authors followed the eclectic approach in developing the model, which is blending a helicopter fuselage and a tilt-rotor wing into a UAM model, which is realistic considering the general layouts shown in Fig. 1. These two components are complemented by a human biodynamics model, coupled to the airframe via a lumped parameter model of a pilot seat. Each component is explained next.

Airframe

The structural dynamics model of a helicopter representative of the Messerschmitt–Bolkow–Blohm (MBB) BO105 has been developed in MASST using the technical data reported in Ref. [12]. This helicopter has been selected because it is considered representative of small-size helicopters, whose payload is similar to that of the UAMs. The six rigid body degrees of freedom and four elastic modes were used to represent the dynamics of the airframe.

Wings

The wing structural data are obtained from XV-15 tilt-rotor models [13]. The available data only allows for modelling the wing as a beam. For this reason, a three-node finite-volume beam formulation [14] in its linear form [15] was used to realize this data as a representative wing. The wings carry four engines (two each), which are assumed to be lumped masses attached to the wing. Each wing was represented by 6 rigid body modes and 6 elastic modes. The data is presented in Table 2.

Table 2: Wing data based on XV-15 tilt-rotor aircraft.

Half-Span^a (m)	5.3
Weight^a (half span) (kg)	575
Out-of-plane bending Stiffness^a (N m^2)	10.7×10^6
Chordwise bending Stiffness^a (N m^2)	32.4×10^6
Torsional Rigidity Stiffness^a (N m^2)	8.1×10^6
Engine Weight^b (kg)	100

a) Ref. [13], *b*) Assumed

Human Body

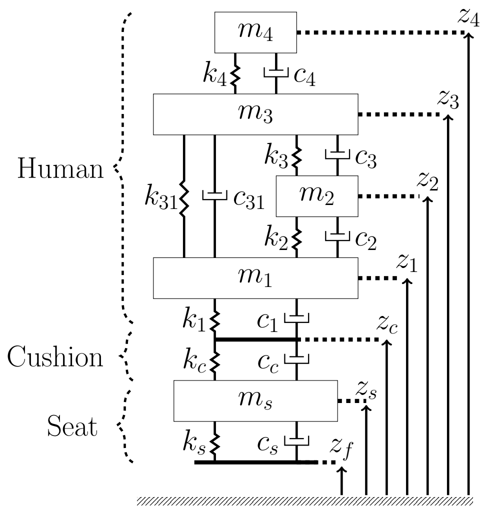

Figure 4: Modified Wan-Schimmels lumped model of a human body [16], seated on a cushion supported by a seat model (from [17]).

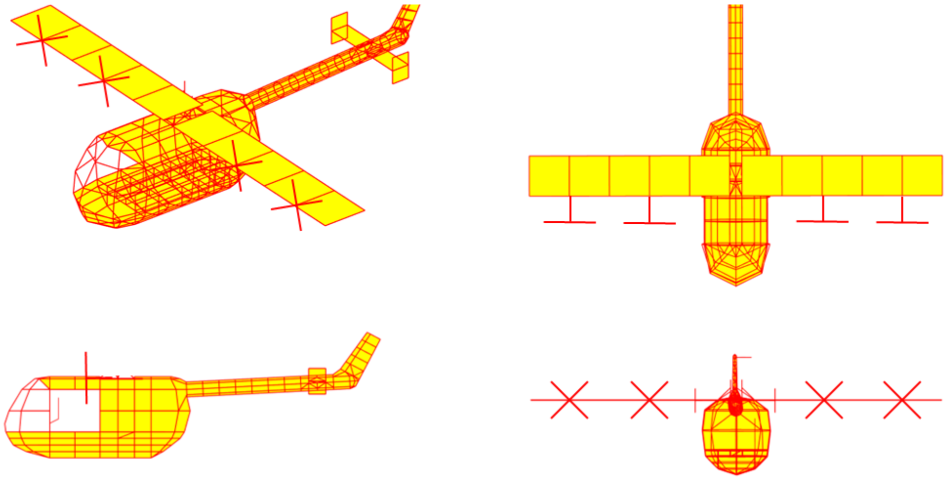

Figure 5: Snapshot of the overall aircraft model.

Comfort guidelines such as ISO-2631 [9] require the evaluation of the acceleration levels of the seat surface. The human body's response to accelerations brings therefore a significant contribution to the seat surface response. The problem can be tackled through the biomechanical modelling of the occupant's body coupled with the vehicle model. In addition, there usually exists a connection element between the subject and the cabin floor, which modifies the level of excitation transferred to their body. In turn, the interface between the structure and human biomechanics feeds loads back to the airframe. This interaction of the vehicle with the interface-human system might affect the magnitude of the accelerations.

Table 3: Numerical values for the Wan-Schimmels [16] and seat-cushion [17] models.

Component	Index	m_i (kg)	c_i ($\mathrm{N\,s\,m^{-1}}$)	k_i ($\mathrm{N\,m^{-1}}$)
Abdomen	i=1	36.00	2475.00	49341.60
Bowels	i=2	5.50	330.00	20000.00
Chest	i=3	15.00	200.00	10000.00
Head	i=4	4.17	250.00	134400.00
Spine	i=31	-	909.09	192000.00
Seat	i=s	13.5	750.00	22600.00
Cushion	i=c	-	159.00	37700.00

Although the proposed method can handle models of increasing complexity originating from different sources, lumped human and seat models are considered here, to provide a sufficiently accurate and generalized infrastructure for vibration rating. This is a reasonable choice since using complex biodynamic modelling techniques does not give significantly different results in comfort assessment [18]. That of Wan and Schimmels [16] is a classical four-degree-of-freedom lumped model of the human body for vibration comfort, in which linear springs and dampers idealize the connections between the body parts. The seat is described as a mass suspended by a spring and damper, whereas the cushion is a massless spring and damper; both are adapted from a helicopter application [17]. The combined seat-human system, as illustrated in Fig 4, was modelled in Matlab as lumped parameter model and coupled to the airframe using three rigid body degrees of freedom and four elastic modes. The numerical values of the parameters are reported in Table 3.

Overall Model

Fig. 5 presents the snapshot of the complete UAM model. The assembly of the wings to the fuselage was realised at the main rotor attachment points of the airframe. The human-seat model was connected to the airframe at a representative pilot location. Since the elements representing the human model are now clearly visible in Fig. 5, a zoomed side-view is given in Fig. 6, including a human body composed of simple shapes. It should be emphasized that multiple human models distributed at different locations in the airframe can be used, also representing passengers and other crew members. Within the scope of this work, a single human biodynamics model representing the pilot was considered.

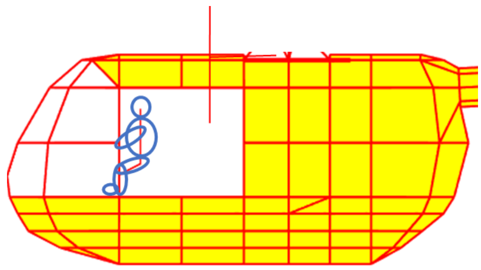

Figure 6: Human biodynamic model location.

Vibratory Loads

An important input in comfort analysis is vibration loading, as this defines the vibration levels. It is connected to comfort rating such as presented in Table 1. In this particular case, propellers are the main source considering that it is the persistent source acting on the occupants throughout the flight, which dominates the weighted acceleration in Eq. 5 over the short-term transient vibrations. On the other hand, obtaining this for the case of propellers requires their aeroelastic modelling, including unsteady aerodynamics. While having an accurate knowledge of the vibratory loads would lead to more realistic results, the amount of work required is beyond the scope of demonstrating a tool for a comfort prediction environment. Therefore, some assumptions are made to conduct the analysis. Two flight conditions were considered: high-speed cruise and transition. For both conditions, the same level of vibratory 1P thrust per engine was assumed, which is 160 N based on 10% of the required thrust level calculated by the equilibrium of lift, weight, thrust and drag. The incidence angle is assumed to be 10 deg for cruise and 45 deg for transition as summarized in Table 4. Both cases are analysed independently rather than being part of a mission profile.

Table 4: Vibratory Loads applied on each engine.

	Cruise	Transition
Angle of Attack (deg.)	10^a	45^a
1P Thrust on engine (N)	160^b	160^b

a) Assumed , b) 10% of cruise thrust

Results and Discussion

The model explained in the previous section was used to demonstrate the suggested method. The vibratory loads are applied at the engines and the acceleration is evaluated at the cushion surface where the pilot is in contact with the seat. Frequency weights are applied and the acceleration level corresponding to ISO-2631 is calculated. The results are interpreted considering Table 1 at three different levels:

- *comfortable*: the weighted acceleration is under 0.03 g, reflecting the 'not uncomfortable' rating;
- *low-comfort*: the weighted acceleration is above 0.03 g and under 0.13 g, combining three intermediate ratings into a single rating;
- *uncomfortable*: the weighted acceleration is greater than 0.13 g, merging the two least comfortable ratings.

The first analysis shows the frequency response of the pilot seat as a function of engine vibratory loads, as presented in Fig. 7. The peaks are the results of the amplification of the motion at the natural frequencies of the overall coupled system, as reported in Table 5. It can be observed that every component contributes to the vibration amplification, justifying the need of using the suggested method, which enables the generation of comprehensive models of combined substructures.

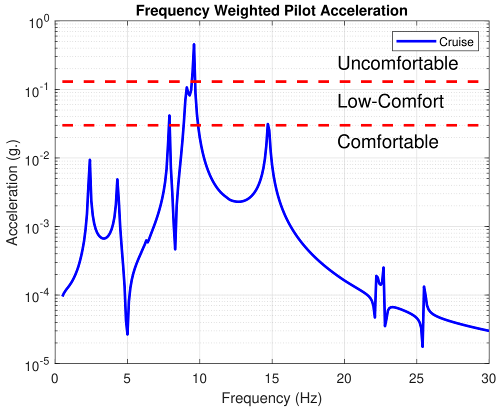

Figure 7: Weighted frequency response of pilot at cruise condition.

Table 5: Modes contributing to peaks in Fig. 7.

Mode	Frequency (Hz)
Seat	2.37
Airframe Vertical Bend.	4.33
Pilot	7.87
Pilot+Airframe	9.07
Pilot+Airframe	9.58
Airframe Vertical Bend. + Wing Bend.	14.70

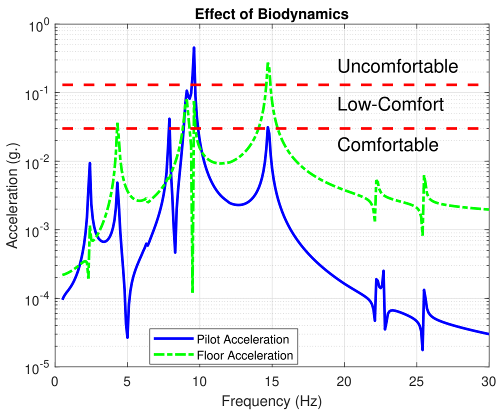

Figure 8: Comparison of pilot seat contact and cabin floor accelerations.

The second curve in Fig. 8 shows the effect of human biodynamics by comparing the seat contact acceleration to that of the floor at the seat' attachment point. The peaks at 7.87 Hz and 47.5 Hz purely result from the human body's dynamic response and would not be there if the pilot were represented as a rigid mass, which could lead to an underestimation of comfort levels. A similar comparison could be made to present the effect of the frequency weights. As can be observed in Fig. 9, frequency weighting can prevent the overestimation of comfort levels at high-frequency excitation. This suggests that moving the dominant vibration sources to higher frequencies with lower human vibration sensitivity can help to improve comfort without the need for changes in aircraft design.

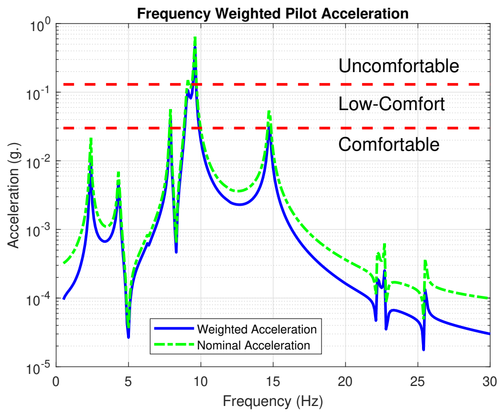

Figure 9: Effect of using ISO-2631 frequency weighting.

Another flight condition with high vibration levels in UAMs is the transition from hover to cruise. The transition phase is a short period in a typical UAM mission, therefore its impact on the overall comfort could be smaller as suggested by Eq. 5. However, the cabin acceleration levels could be higher than the cruise due to high incidence angles causing complex flow field and the vertical attitude of the thrust vector exciting vertical modes. Therefore, the transient phase can have a detrimental effect on the public acceptance of UAMs if it is not properly addressed. Fig. 10 presents the frequency-weighted acceleration of the pilot at the seat surface for both cruise and transition flights for the same amplitude of vibratory thrust force. The curves suggest that transition flight leads to some discomfort at the lower end of the spectrum.

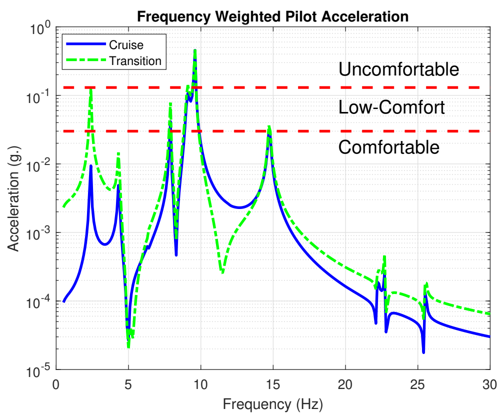

Figure 10: Comparison of the comfort levels during the transition and cruise for the same level of vibratory thrust amplitude.

The final set of analyses presents the RPM change in one of the propellers and its effect on the weighted acceleration. If rotors can rotate at different speeds (i.e., without mechanical interconnection), and thrust is controlled via rpm change, there could be beating problems. In this case, vibrations at different but close frequencies would combine and get much higher when in phase. Such a condition was analysed by changing the RPM of engines one by one about a nominal RPM, which was set at 10 Hz. Both negative and positive changes were considered.

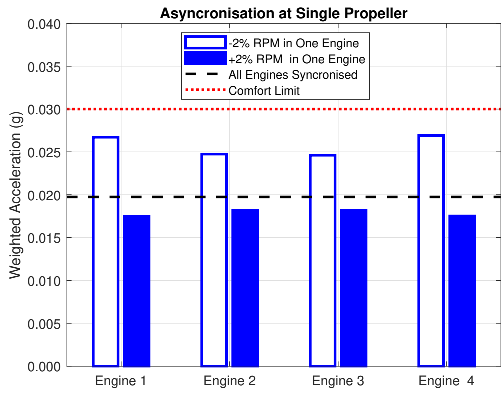

Figure 11: Effect of non-synchronisation in each engine on comfort levels at 10 Hz nominal RPM and a 2% deviation.

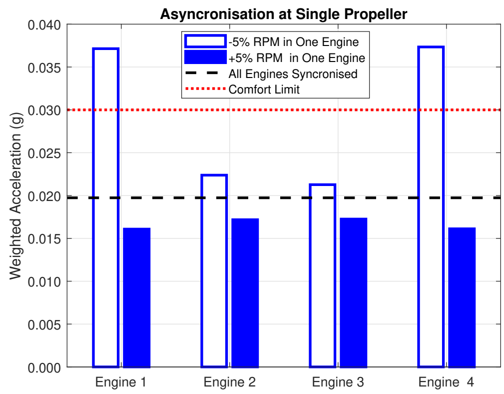

Figure 12: Effect of non-synchronisation in each engine on comfort levels at 10 Hz nominal RPM and a 5% deviation.

Fig. 11 and Fig. 12 respectively show the results for the 2% and 5% change in RPM. The results are presented as follows: i) the blue hollow bars represent a reduction in RPM; ii) the blue filled bars correspond to the reduction in RPM; iii) the black dashed line shows the synchronised vibration level; and iv) the red dotted line presents the comfort limit. It can be observed from the two figures that the reduction of RPM in a single engine increases the comfort level. The opposite happens when the RPM is increased. This is in line with the behaviour observed in Fig. 7, which shows a steep change in vibrational level at about 10 Hz. Another conclusion from the results is that a high enough change in the RPM in a single engine can lead to an uncomfortable ride on an otherwise comfortable aircraft. This suggests that UAM comfort level assessment should include such analysis if the engines are independently powered/driven.

Conclusions

This paper discussed the use of a modular simulation environment for the use of UAM comfort analysis. A mid-fidelity model was built by combining a modal reduction of an FE model of the airframe, a beam model of the wing with four engines attached as equivalent masses and inertia properties, and a human biodynamics model. ISO 2631 comfort standard was considered to reflect the human perception of vibration in the analysis. Through analysis, the benefit of using the tool in UAM comfort prediction was demonstrated. The authors believe that UAM design can largely benefit from the proposed method, with its modular characteristics that support preliminary comfort assessment from early design phases.

The core aspect of this work is to develop the framework and demonstrate its use, as successfully presented. Nonetheless, the authors are aware of some of its shortcomings. Indeed, the model considered in this work is a combination of an airframe obtained from a helicopter and a wing from a tiltrotor aircraft. Therefore, the analysis was not applied to a dedicated UAM design. The second one is the vibratory forcing amplitude, which was estimated through vaguely defined assumptions. Although the authors are confident of the validity of the proposed analysis in terms of methodology, its application to more realistic models will be the subject of future work.

Copyright Statement

References

[1] Air Transport Action Group. Waypoint 2050: An air transport action group project. Report, Air Transport Action Group., 2020.

[2] Wayne Johnson. *Rotorcraft Aeromechanics*. Cambridge University Press, New York, 2013.

[3] A.C. Veca. Vibration effects on helicopter reliability and maintainability. TM 73-11, NASA, 1973.

[4] Jessica K. Ljungberg and Gregory Neely. Stress, subjective experience and cognitive performance during exposure to noise and vibration. *Journal of Environmental Psychology*, 27(1):44 – 54, 2007.

[5] Siena K. S. Whiteside, Beau P. Pollard, Kevin R. Antcliff, Nikolas S. Zawodny, and Xiaofan Fei. Design of a tiltwing concept vehicle for urban air mobility. TM 20210017971, NASA, 2021.

[6] Aykut Tamer, Vincenzo Muscarello, Pierangelo Masarati, and Giuseppe Quaranta. Evaluation of vibration reduction devices for helicopter ride quality improvement. *Aerospace Science and Technology*, 95:105456, 2019.

[7] Pierangelo Masarati, Vincenzo Muscarello, and Giuseppe Quaranta. Linearized aeroservoelastic analysis of rotary-wing aircraft. In *36th European Rotorcraft Forum*, pages 099.1–10, Paris, France, September 7–9 2010.

[8] Roy R. Craig, Jr. and Mervyn C. C. Bampton. Coupling of substructures for dynamic analysis. *AIAA Journal*, 6(7):1313–1319, July 1968.

[9] ISO. ISO mechanical vibration and shock - evaluation of human exposure to whole-body vibration. Technical Report ISO2631-1, ISO, 1997.

[10] Aykut Tamer, Vincenzo Muscarello, Giuseppe Quaranta, and Pierangelo Masarati. Cabin layout optimization for vibration hazard reduction in helicopter emergency medical service. *Aerospace*, 7(5), 2020.

[11] W. Johnson and C. Silva. Nasa concept vehicles and the engineering of advanced air mobility aircraft. *The Aeronautical Journal*, 126(1295):59–91, 2022.

[12] O. Dieterich, J. Götz, B. DangVu, H. Haverdings, P. Masarati, M. D. Pavel, M. Jump, and M. Gennaretti. Adverse rotorcraft-pilot coupling: Recent research activities in Europe. In *34th European Rotorcraft Forum*, Liverpool, UK, September 16–19 2008.

[13] C. W. Acree, R. J. Peyran, and Wayne Johnson. Rotor design options for improving tiltrotor whirl-flutter stability margins. *Journal of the American Helicopter Society*, 46(2):87–95, April 2001. doi:10.4050/JAHS.56.022004.

[14] Gian Luca Ghiringhelli, Pierangelo Masarati, and Paolo Mantegazza. A multi-body implementation of finite volume beams. *AIAA Journal*, 38(1):131–138, January 2000. doi:10.2514/2.933.

[15] Aykut Tamer and Pierangelo Masarati. Linearized structural dynamics model for the sensitivity analysis of helicopter rotor blades. In *Ankara International Aerospace Conference*, Ankara, TR, September 11–13 2013.

[16] Y. Wan and J. M. Schimmels. Optimal seat suspension design based on minimum simulated subjective response. *Journal of biomechanical engineering*, 119(4):409–416, 1997.

[17] Young-Tai Choi and Norman Wereley. Biodynamic response mitigation to shock loads using magnetorheological helicopter crew seat suspensions. *Journal of Aircraft*, 42(5):1288–1295, 2005.

[18] Aykut Tamer, Andrea Zanoni, Vincenzo Muscarello, Alessandro Cocco, Giuseppe Quaranta, and Pierangelo Masarati. Biodynamic modeling techniques for rotorcraft comfort evaluation. *Aerotecnica Missili & Spazio*, June 2019.